

Catalysis Science & Technology

Accepted Manuscript



This is an *Accepted Manuscript*, which has been through the Royal Society of Chemistry peer review process and has been accepted for publication.

Accepted Manuscripts are published online shortly after acceptance, before technical editing, formatting and proof reading. Using this free service, authors can make their results available to the community, in citable form, before we publish the edited article. We will replace this *Accepted Manuscript* with the edited and formatted *Advance Article* as soon as it is available.

You can find more information about *Accepted Manuscripts* in the [Information for Authors](#).

Please note that technical editing may introduce minor changes to the text and/or graphics, which may alter content. The journal's standard [Terms & Conditions](#) and the [Ethical guidelines](#) still apply. In no event shall the Royal Society of Chemistry be held responsible for any errors or omissions in this *Accepted Manuscript* or any consequences arising from the use of any information it contains.

Cite this: DOI: 10.1039/c0xx00000x

www.rsc.org/xxxxxx

ARTICLE TYPE

Asymmetric epoxidation of unfunctionalized olefins accelerated by thermoresponsive self-assemblies in aqueous system

Yaoyao Zhang,^a Rong Tan,^{*a} Guangwu Zhao,^a Xuanfeng Luo^a and Donghong Yin^{*a,b}

Received (in XXX, XXX) Xth XXXXXXXXX 200X, Accepted Xth XXXXXXXXX 200X

DOI: 10.1039/b000000x

A novel thermoresponsive surfactant-type chiral salen Mn^{III} catalyst was developed by axially grafting “smart” poly(Nisopropylacrylamide) (PNIPAAm) onto metal center of a neat chiral salen Mn^{III} complex. Characterization suggested the thermoresponsive micellization behavior of obtained catalyst in water. The chiral metallomicellar catalyst acted as nanoreactor to carry out asymmetric epoxidation of unfunctionalized olefins in water and dramatically accelerated the reaction rates. Outstanding catalytic efficiency was observed in the nanoreactor system. In particular, quantitative conversion (99%) of styrene with high enantioselectivity (39%) was achieved over 0.8 mol% of the catalyst within even 3 min, giving an unprecedented TOF value ($2.48 \times 10^3 \text{ h}^{-1}$) which was significantly higher than that obtained over previously reported homogeneous or heterogeneous systems. Moreover, the catalyst could be easily recovered by thermocontrolled separation and be reused with high activity for five cycles.

Introduction

Asymmetric epoxidation of unfunctionalized alkenes catalyzed by chiral salen Mn^{III} complexes is of great importance in synthetic organic chemistry, since the obtained enantiopure epoxides are useful chiral intermediates for synthesizing fine chemicals and several pharmaceuticals.¹⁻⁶ Industrial practice however is limited to the use of volatile dichloromethane as a solvent which often results in environmental problem. Reactions using water as a reaction medium are attracting much attention, because water is inexpensive, safe and environmentally benign.⁷⁻¹¹ More importantly, water often exerts a synergistic effect on chemical reactivity and selectivity.^{12,13} While, to the best of our knowledge, few reports have focused on efficiently performing this transformation in water because of the insolubility of substrate and catalyst. An efficient way to address this issue is to introduce surfactant additives or to use surfactant-like catalysts.¹⁴⁻¹⁶ Generally, amphiphilic surfactants can self-assemble in water via the interaction between hydrophobic blocks, spontaneously forming micelles with hydrophilic surfaces and hydrophobic cores. Hydrophobic reactants are concentrated within the core through hydrophobic affinity, resulting in the observed

acceleration in reaction rate.^{14, 17-21} The pre-organizing function of surfactants in aqueous organic reactions encouraged us to envision that a surfactant-type chiral salen Mn^{III} complex obtained by introducing a hydrophilic block to a chiral salen Mn^{III} complex should efficiently catalyze asymmetric epoxidation of alkenes in water. Upon self-assembly, hydrophobic chiral salen Mn^{III} complex segment confined in the core domain can be forced into highly dense arrangements. Hydrophobic affinity of core for reactants also favors the migration of hydrophobic substrates from aqueous medium. High concentration of catalyst and substrate localized within a confined hydrophobic space was expected to accelerate the asymmetric epoxidation.

However, traditional micelles are difficult to recover from solution due to amphiphilic nature. An ideal solution to this problem is to develop “stimuli-responsive” micelles that can undergo inverse solubility changes in response to local environment changes. Temperature sensitivity is one of the most interesting properties for “stimuli-responsive” micelles. Polymeric N-isopropylacrylamide (PNIPAAm), with the lower critical solution temperature (LCST, 32 °C) close to room temperature, is an attractive thermoresponsive polymer.²²⁻²⁵ The thermoresponsive behavior, that is able to undergo hydrophilic-to-hydrophobic transformation as temperature increases, make it a promising modifier to fabricating thermoresponsive surfactant-type chiral salen Mn^{III} complex for asymmetric epoxidation of alkenes in water. At the reaction temperature (2 °C), catalyst incorporating the hydrophobic chiral salen Mn^{III} complex along with the hydrophilic PNIPAAm moiety behaves as a surfactant to form micelles-based nanoreactor in water. After the reaction, it can reversibly switch to a double hydrophobic block once heated above its LCST, leading to collapse and precipitation of the catalyst for facile recovery. This switchable behavior allows for a

^a Key Laboratory of Chemical Biology and Traditional Chinese Medicine Research (Ministry of Education), Key Laboratory of the Assembly and Application for Organic Functional Molecules, Hunan Normal University, Changsha, Hunan, 410081, China;

^b Technology Center, China Tobacco Hunan Industrial Corporation, NO. 426 Laodong Road, Changsha, Hunan, 410014, China.

Fax: +86-731-8872531; Tel: +86-731-8872576; E-mail: yiyangtanrong@126.com (R. Tan) or yindh@hunnu.edu.cn (D. Yin)

typical homogeneous reaction coupled with heterogeneous separation in the aqueous asymmetric epoxidation.

Herein, thermoresponsive surfactant-type chiral salen Mn^{III} complex (denoted as **catalyst 1**) was prepared by axially grafting thermoresponsive PNIPAAm onto the metal center of a neat chiral salen Mn^{III} complex under basic conditions. The axial grafting mode, which does not need to tune the structures of chiral salen Mn^{III} and PNIPAAm moiety, not only represents a simple and facile process, but also minimizes the formation of undesired inactive dimeric μ -oxo-manganese(IV) dimers due to steric crowding at metal center. It has proved that the catalyst could self-assemble to form nanoreactor in asymmetric epoxidation of unfunctionalized olefins in water, dramatically accelerating the aqueous epoxidation. Furthermore, it could be easily recovered from the reaction system through thermocontrolled separation. Activity switching was repeatable even after five heating/cooling cycles. Thus, the problems associated with the mass transfer and recovery limitation of chiral salen Mn^{III} complex in asymmetric epoxidation of unfunctionalized olefins in water can be well resolved.

Experimental Section

Materials and reagents

N-Isopropylacrylamide (NIPAAm) was provided by Acros, and was purified by recrystallization from *n*-hexane and dried at 25 °C in vacuo. N,N-Azobis(isobutyronitrile) (AIBN), 2-aminoethanethiol hydrochloride and L(+)-tartaric acid were also purchased from Acros. 2-tert-Butyl phenol was purchased from Alfa Aesar. Pyridine-N-oxide (PyNO) was bought from Aldrich. Indene and 1,2-dihydronaphthalene were obtained by TCI. Other commercially available chemicals were laboratory grade reagents from local suppliers. All solvents employed in the reactions were distilled from appropriate drying agent prior to use. Organic solutions were concentrated under reduced pressure on a rotary evaporator. Styrene and indene were passed through a pad of neutral alumina before use. Amino-terminated PNIPAAm (PNIPAAm-NH₂) was prepared by radical polymerization using thiol compounds as a chain transfer agent according to the procedure described in the literature.²⁶ The neat complex of [(R,R')-(N,N'-bis (3,5-di-tert-butylsalicylidene)-1,2-cyclohexanediaminato) manganese(III)-chloride was prepared according to the described procedure.²⁷

Methods

Number-average molecular weight (M_n) of PNIPAAm was obtained by gel permeation chromatograph (GPC). Analyses were performed on an Alltech Instrument (Alltech, America) using THF as the solvent eluting at a flow of 1 mL min⁻¹ through a Jordi GPC 10000 A column (300 mm×7.8 mm) equipped with an Alltech ELSD 800 detector. The system was calibrated with standard polystyrenes. The detection temperature is 40 °C and column temperature is 30 °C. ¹H NMR spectra of samples was recorded at a Varian-500 spectrometer. FT-IR spectra were obtained as potassium bromide pellets with a resolution of 4 cm⁻¹ and 32 scans in the range 400–4000 cm⁻¹ using an AVATAR 370 Thermo Nicolet spectrophotometer. UV-vis spectra of complex were obtained on a UV-vis Agilent 8453 spectrophotometer at 300–600 nm. The lower critical solution temperature (LCST) of

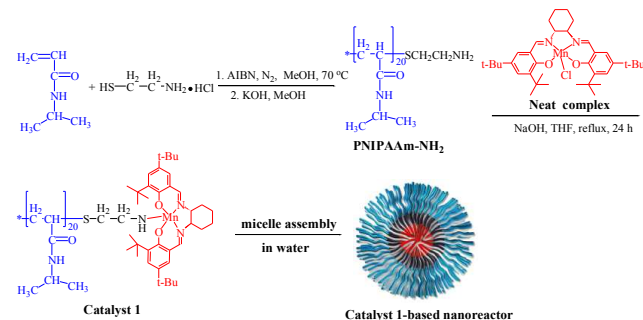
the thermoresponsive chiral salen Mn^{III} complex in water was measured by transmittance using a UV-visible photometer. The concentration of complex is 1 wt%. The rising temperature ratio is 5 °C min⁻¹. X-ray Photoelectron Spectroscopy (XPS) data were obtained with an ESCALab220i-XL electron spectrometer from VG Scientific using 300 W Al K α radiation. The base pressure was about 3×10^{-9} mbar (3×10^{-7} Pa). The manganese content in catalyst was determined by inductively coupled plasma-atomic emission spectrometry (ICP-AES) on a BAIRD PS-6 analyzer, after the sample was dissolved in deionized water. The optical rotation of catalysts was measured in dichloromethane on a WZZ-2A Automatic Polarimeter. Surface tension of aqueous solution of **catalyst 1** was measured as a function of catalyst concentration (3.75×10^{-2} –500.0 mmol L⁻¹) on a Krüss K12 tensiometer by using Wilhelmy plate method at 25 °C. The surface tension vs. catalyst concentration plot gives information on the critical micelle concentration (CMC). Morphological observation of the micelles was performed by TEM on a Microscope JEM-2100F at an accelerating voltage of 200 kV. Sample was prepared by depositing aqueous solution of **catalyst 1** (0.5 mg mL⁻¹) onto a carbon-coated copper grid, followed by removal of excess solution by blotting the grid with filter paper. The samples were dried for 72 h at room temperature in a desiccator containing dried silica gel. After that, the samples were negatively stained by phosphotungstic acid and dried for another 72 h before examination. The average hydrodynamic diameter and size distribution of self-assembled aggregates were determined by dynamic light scattering (DLS) using a MS2000 Laser Particle Size Analyzer (Malvern, UK). The concentration of the sample was 0.5 mg/mL. Light transmittance was fixed at 633 nm with the scattering angle of 90°.

Preparation of Catalyst 1

The preparation of **catalyst 1** was outlined in Scheme 1.

Synthesis of PNIPAAm-NH₂: NIPAAm (50 mmol), 2-aminoethanethiol hydrochloride (1 mmol) and AIBN (0.5 mmol) were dissolved in 20 mL of methanol in a Schlenk tube. The reaction mixture was degassed by bubbling with nitrogen gas at room temperature for 30 min, and polymerization was carried out at 70 °C for 5 h under a N₂ gas atmosphere. The mixture was cooled to room temperature, and then treated with KOH (1 mmol). The obtained solution was concentrated under vacuum and then poured into diethyl ether to precipitate the polymer. The crude product was further purified by repeated precipitation from a THF solution into diethyl ether to remove unreacted monomers, and then dried for 12 h under a vacuum at 25 °C to give a white solid of PNIPAAm-NH₂. FT-IR (KBr): $\gamma_{\max}/\text{cm}^{-1}$ 3438, 3309, 3072, 2974, 2931, 2878, 2825, 1652, 1541, 1458, 1387, 1367, 1261, 1173, 1130, 1055, 987, 928, 881, 839, 633, 517 cm⁻¹. ¹H NMR (500 MHz, D₂O): δ 3.89 (s, 20H), 2.92 (s, 12H), 2.62 (s, 1H), 2.44 (s, 1H), 2.00 (s, 20H), 1.57 (s, 42H), 1.14 (s, 123H). The M_n of the PNIPAAm-NH₂ was ca. 2300 g/mol, which was measured by GPC using conventional calibration with PS standards. Thus, the polymer was comprised in ca. 20 repeating units of NIPAAm monomer.

Synthesis of catalyst 1: A solution of neat chiral salen Mn^{III} complex (2.7 mmol, 1.71 g), PNIPAAm-NH₂ (2.5 mmol) and adequate amount of sodium hydroxide in THF (50 mL) was vigorously stirred for 24 h under reflux. After removing THF, the



Scheme 1. Schematic representation of synthesis and self-assembly of surfactant-type **catalyst 1**.

residue was purified by precipitation from diethyl ether (3×50 mL), dried in vacuo under a vacuum at 25 °C to get the thermoresponsive surfactant-type catalyst (denoted as **catalyst 1**). FT-IR (KBr): $\gamma_{\max}/\text{cm}^{-1}$ 3309, 3072, 2974, 2931, 2878, 1652, 1541, 1458, 1387, 1365, 1254, 1173, 1130, 928, 879, 837, 644, 571, 507, 424 cm^{-1} . UV-vis (CH₂Cl₂): λ_{\max}/nm ($\epsilon_{\max}/\text{L}\cdot\text{mol}^{-1}\cdot\text{cm}^{-1}$) 322 (148162), 429 (32119), 502 (5963). Mn ion content: 0.33 mmol/g (theoretical value: 0.34 mmol/g). $\alpha_{\text{D}}^{25} = +168$ (C = 0.02 in CH₂Cl₂). The LCST of **complex 1** in aqueous solution was ca. 35 °C, which was determined by transmittance measurements using the UV-vis spectrophotometer.

Catalyst testing

Unfunctionalized alkene (0.25 mmol) and PyNO (0.5 mmol, 0.048 g) were added into the solution of catalyst (0.8 mol% of substrate, based on Mn content) in water (1 mL) at 2 °C. Buffered NaOCl as an oxidant (0.5 mmol, 0.5 M, pH=11.5) was then added in one portion under stirring. The reaction was monitored constantly by TLC. After achieving the desired epoxidation level, the reaction mixture was heated to 40 °C. Catalyst was precipitated out from the reaction system, washed with *n*-hexane (3×5 mL), dried in a vacuum, and finally recharged with fresh substrate, additive, and oxidant for the next catalytic cycle. The supernatants separated from reaction system were extracted with *n*-hexane thrice. Further purification of the collected *n*-hexane phase by flash column chromatography afforded epoxides. The conversion and enantiomeric excess (ee) were determined by a 6890N gas chromatograph (Agilent Co.) equipped with the chiral capillary column (HP19091G-B213, 30 m×0.32 mm×0.25 μm) and the FID detector. Nitrogen was used as the carrier gas with a flow of 30 mL min⁻¹. The injector temperature is 250 °C, and the detector temperature is also 250 °C. The retention times of the corresponding chiral epoxides (*t*_{absolute configuration}) are as follows: (a) styrene epoxide: the column temperature is 100 °C, major enantiomer *t*_R = 7.1 min and minor enantiomer *t*_S = 7.6 min; (b) α -methylstyrene epoxide: the column temperature is 100 °C, major enantiomer *t*_R = 8.0 min and minor enantiomer *t*_S = 7.7 min; (c) indene epoxide: the column temperature was programmed from 80 to 180 °C with 5 °C·min⁻¹. Major enantiomer *t*_{RS} = 11.9 min and minor enantiomer *t*_{SR} = 11.5 min; (d) 1,2-dihydronaphthalene epoxide: the column temperature was programmed from 80 to 180 °C with 5 °C min⁻¹. Major enantiomer *t*_{RS} = 19.4 min and minor enantiomer *t*_{SR} = 18.8 min; (e) 6-nitro-2,2'-dimethylchromene epoxide: the column temperature was programmed from 80 to 200 °C with 3 °C min⁻¹ and retained at

200 °C for 5 min. Major enantiomer *t*_{RR}=30.8 min and minor enantiomer *t*_{SS}=30.3 min; (f) 6-cyano-2,2'-dimethylchromene epoxide: the column temperature was programmed from 80 to 200 °C with 4 °C·min⁻¹. Major enantiomer *t*_{RR} = 24.3 min and minor enantiomer *t*_{SS} = 24.0 min.

Epoxidation reaction for kinetic measurements

A cooled solution of **catalyst 1** in water (1 mL) was stirred with styrene (0.25 mmol). Buffer NaOCl (0.5 mmol, 1 mL, pH = 11.5) was then added into the stirred solution in one portion at 2 °C. To determine the rate of epoxidation, aliquots at an interval of 1 min were drawn from the reaction mixture, quenched with triphenylphosphine, and analyzed on GC.

Results and Discussion

Preparation and Characterization of Catalysts

Nanometer-scale reactors that mimic enzymes-based reaction compartments have drawn much attention in recent years, since they provide an opportunity to perform organic reactions “in water”.²⁸⁻³¹ Surfactant-type catalysts can spontaneously self-assemble in water to form micelles-based nanoreactors, and hopefully accelerated the aqueous organic reaction.^{15,32} Therefore, we decided to develop a surfactant-type chiral salen Mn^{III} complex for efficient asymmetric epoxidation of unfunctionalized alkenes in water. PNIPAAm with inverse temperature-dependent water solubility was introduced into the structure of chiral salen Mn^{III} complex for this development. Axial grafting mode, a common way to heterogenize chiral salen Mn^{III} complex which does not need to tune the structure of chiral salen Mn^{III} complex,³³ was employed for this modification. It not only represents a simple and facile process, but also ensures the effective site isolation due to steric crowding at metal center, since catalyst density and site isolation are the key issues in giving extremely active and selective chiral salen Mn^{III} catalysts.³³ The synthesis route for the thermoresponsive catalyst is outlined in Scheme 1. Amino-terminated PNIPAAm, prepared by radical polymerization using thiol compounds as a chain transfer agent, directly reacted with neat chiral salen Mn^{III} complex under a basic condition, affording the **catalyst 1**.

Characterization of Samples

FT-IR

The obtained **catalyst 1**, as well as the PNIPAAm and neat chiral complex for comparison, were characterized by FT-IR spectra (Fig. 1). PNIPAAm exhibited characteristic vibration bands at around 3309 cm^{-1} (–NH of –CONH–), 3072 cm^{-1} (CH of –CH–CH–), 2974, 2931 cm^{-1} (–CH₃ of –CH (CH₃)₂), 2878 cm^{-1} (CH of –CH (CH₃)₂) and 1652 cm^{-1} (–C=O of –CONH–) (Fig. 1a) in the FT-IR spectrum.³⁴ Upon grafting, new characteristic bands at around 1251, 571, and 424 cm^{-1} appeared along with the characteristic vibration bands associated with PNIPAAm (Fig. 1b), which were assigned to the characteristic vibrations of Ph–O, Mn–O, and Mn–N in the salen Mn^{III} unit,³⁵⁻³⁷ respectively. Obviously, the structure of chiral salen Mn^{III} complex was maintained in **catalyst 1**. Notably, the characteristic vibrations of Mn–O and Mn–N shifted from 565 and 413 cm^{-1} to

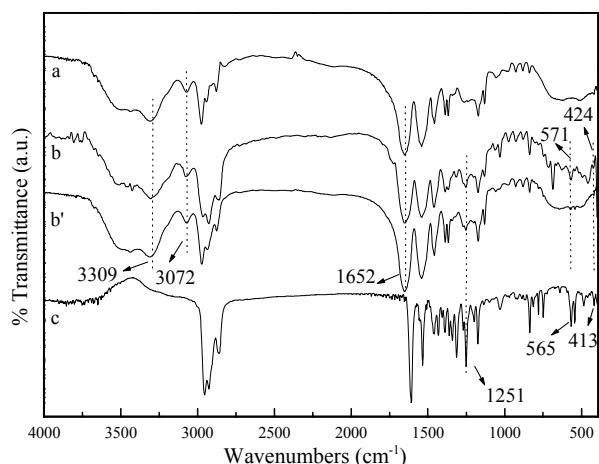


Fig. 1 FT-IR spectra of PNIPAAm (a), fresh **catalyst 1** (b), recovered **catalyst 1** after the 5th reuse (b') and neat complex (c).

5 571 and 424 cm^{-1} , respectively, after grafting, compared with those of the neat chiral salen Mn^{III} complex (Fig. 1b vs. 1c). This slight shift should account for the interaction between metal center of chiral salen Mn^{III} complex and amino-terminated PNIPAAm. It is the interaction that responsible for axially
10 bonding PNIPAAm- NH_2 to the chiral salen Mn^{III} complex.

UV-vis

UV-vis spectra of neat complex and **catalyst 1** in dichloromethane furthermore verified the interaction between metal center of chiral salen Mn^{III} complex and amino-terminated
15 PNIPAAm, as described in Fig. 2. Obviously, neat complex exhibited the characteristic peaks at around 325, 438 and 509 nm (Fig. 2a), which was due to charge transfer transition of salen ligand, metal-to-ligand charge-transfer transition and d-d transition of complex, respectively.³⁵ As for **catalyst 1**, the
20 corresponding characteristic peaks shifted to 322, 429 and 502 nm, respectively (Fig. 2a vs 2b). It was logical to relate the blue shift with electronegative nitrogen atom bonded on the manganese center in **catalyst 1**. Similar deduction has also been made by Huang et al.^{38, 39} They reported an axial N-Mn bonding
25

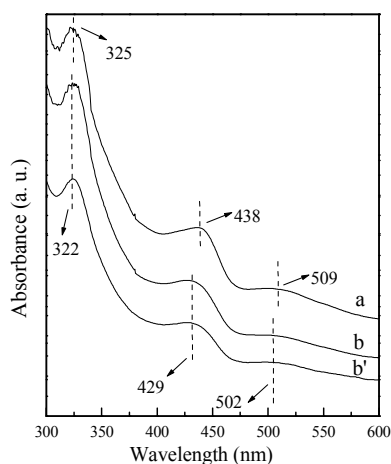


Fig. 2 UV-vis spectra of neat complex (a), fresh **catalyst 1** (b), recovered **catalyst 1** after the 5th reuse (b').

between chiral salen Mn^{III} complex and amine ($-\text{NH}_2$) group
30 modified supports. The observations provided a direct proof for the presence of N-Mn bonding in **catalyst 1**. PNIPAAm was thus axially appended on the manganese center of chiral salen Mn^{III} complex through the terminal amine ($-\text{NH}_2$) group, which not only acted as a thermoresponsive inductor to switch on and off
35 the nanoreactor, but also behaved as a bulk axial group to ensure the necessary isolation of active site.

XPS

The binding behavior can also be confirmed by characterizing neat complex and **catalyst 1** using XPS, since the electronic
40 environment influences the binding energy of the core electrons of the metal. XPS spectra obtained from the neat complex and **catalysts 1** were shown in Fig. 3. Neat complex exhibits $\text{Mn}2p_{3/2}$ core level peak at a binding energy of 642.0 eV, in accordance with earlier literature value.⁴⁰ While, the binding energy slightly
45 increases to 642.4 eV in the case of **catalyst 1**. The observed increase of binding energy should attribute to the formed N-Mn bonding in **catalyst 1**, which affected the electronic environment of manganese center. A similar observation has also been made for a chiral salen Mn^{III} catalyst which was axially grafted on
50 amine ($-\text{NH}_2$) groups modified supports through a N-Mn bonding.⁴¹

CMC Determination

CMC is one of the most useful parameters for surfactant- type **catalyst 1**, since the catalyst can self-assemble to form micelles
55 above the CMC.⁴² Surface tension measurement over a wide range of concentrations was used in the CMC determination. Fig. 4 showed the surface tension versus logarithm of concentration plots for **catalyst 1** in water at 25 °C. Clearly, the surface tension decreased dramatically as concentration of **catalyst 1** increased.
60 While, there was an inflection point at the characteristic concentration of 0.5 $\text{mmol} \cdot \text{L}^{-1}$. And the surface tension does not change substantially as a function of concentration of **catalyst 1** above 0.5 $\text{mmol} \cdot \text{L}^{-1}$. Therefore, the CMC of **catalyst 1** is 0.5 $\text{mmol} \cdot \text{L}^{-1}$, above which, **catalyst 1** could self-assemble in water
65 to form micelles.

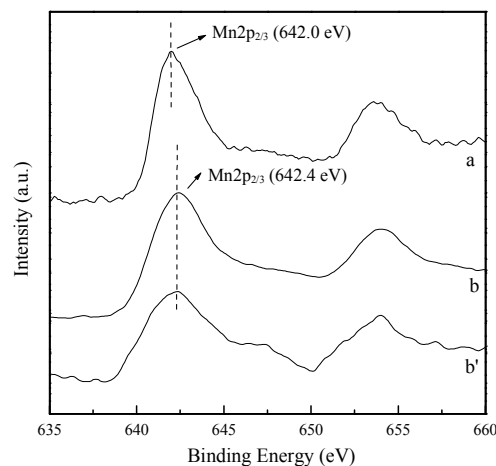


Fig. 3 $\text{Mn} 2p_{3/2}$ XPS spectra of neat complex (a), fresh **catalyst 1** (b), recovered **catalyst 1** after the 5th reuse (b').

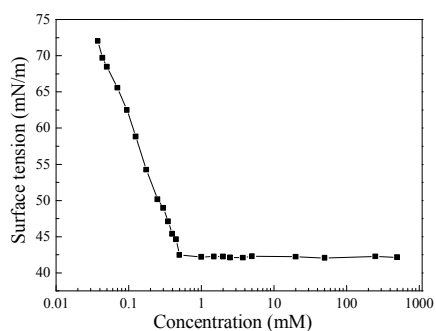


Fig. 4 Plot of surface tension against logarithm of concentration for **catalyst 1** in water at 25 °C.

5 Morphological analyses

TEM measurement was employed to observe the morphology of the micelles, as shown in Fig. 5. Obviously, **catalyst 1** self-assembled in water to form spherical aggregates with an average diameter of *ca.* 9 nm, as confirmed by TEM. High dispersion of the aggregates suggested the stability of micelles in water. In order to further determine the hydrodynamic diameter and size distribution the self-assembled aggregates, **catalyst 1** in water (0.5 mg. mL⁻¹) was measured by a MS2000 Laser Particle Size Analyzer (Fig. 6). Indeed, the micelles showed a narrow diameter distribution with average diameter of 78 nm. Notably, the size obtained from DLS is much greater than that from TEM (*ca.* 9 nm), probably due to the swell of surface PNIPAAm in aqueous solution. In fact, DLS allows determining the hydrodynamic diameter of micelles in water, whereas TEM shows the dehydrated solid state of dried micelles. Furthermore, homogeneous distribution and spherical morphology of the self-assemblies led to a small polydispersity index (PDI) value of 0.282.⁴³

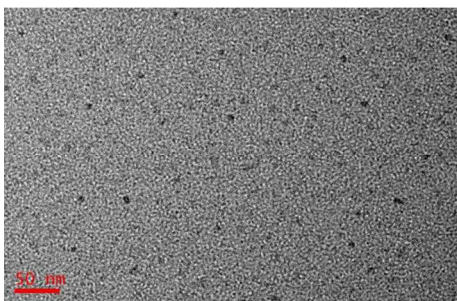


Fig. 5 TEM micrograph of self-assembled **catalyst 1** stained with phosphotungstic acid.

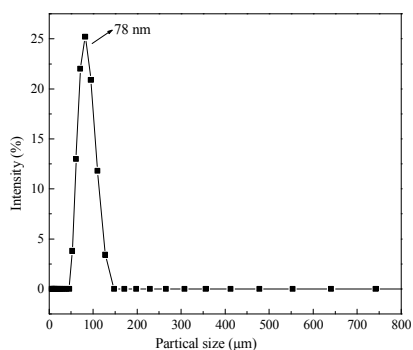


Fig. 6 Hydrodynamic diameter of self-assembled **catalyst 1** (PDI=0.282).

LCST Determination

The thermal sensitivity of these micelle structures was measured *via* spectrophotometry by determining the turbidity of a solution at various temperatures (Fig. 7). A sharp decrease in transmittance occurred at *ca.* 35 °C, which signified a hydrophilic-to-hydrophobic phase transition of PNIPAAm block (Fig. 7a). Therefore, **catalyst 1**-based micelles were formed when local temperature was below 35 °C and disaggregated at temperature above 35 °C. Furthermore, the LCST of **catalyst 1** (35 °C) was 3 °C higher than that for PNIPAAm (32 °C) (Fig. 7a vs 6b). This trend may be attributed to the interaction between chiral salen Mn^{III} complex moiety and PNIPAAm component.

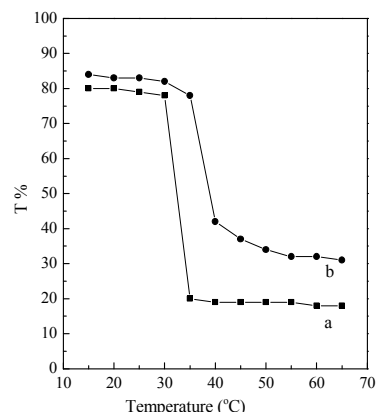


Fig. 7 Plot of the changes in solution transmittance as a function of temperature for PNIPAAm (a) and **catalyst 1** (b) solution in water. The turbidimetry curve is drawn by measuring the transmittance ($\lambda_{\text{max}} = 450$ nm) of the corresponding aqueous polymer solution at a fixed concentration (5 mg. mL⁻¹) as a function of temperature. The LCST corresponds to the mid-point of the transition curve.

Catalytic Performances

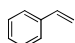
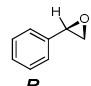
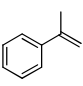
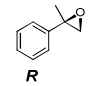
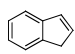
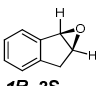
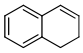
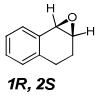
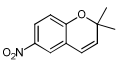
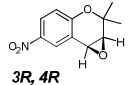
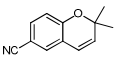
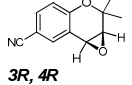
The **catalyst 1**-based micelles behaved as catalytic nanoreactors for asymmetric epoxidation of alkenes in water. Styrene was chosen as a model substrate to investigate the catalytic performance of **catalyst 1** in pure water. All catalytic reactions were conducted at 2 °C to ensure the formation of nanoreactor with hydrophilic surface and hydrophobic catalytic core during reaction. The results are presented in Table 1.

As expected, **catalyst 1** was extremely efficient for the asymmetric epoxidation of styrene in water. Quantitative conversion (99%) with high enantioselectivity (ee, 39%) was achieved over 0.8 mol% of **catalyst 1** even within 3 min (Table 1, entry 1). While, only 16% conversion of styrene with 5% ee value was obtained over neat complex under identical conditions (Table 1, entry 3). Notably, PNIPAAm alone was inactive (Table 1, entry 4). Therefore, the unprecedented acceleration in reaction rate (six times faster than neat complex) should relate to micellization behavior of **catalyst 1** in reaction system. During the reaction, **catalyst 1** containing hydrophobic and hydrophilic blocks spontaneously self-assembled in water to form micelles with hydrophobic catalytic core and hydrophilic surface. Hydrophobic core provided a hydrophobic microenvironment with high local concentration of catalytic sites along with the

concentrated hydrophobic substrates, while the hydrophilic surface guaranteed water-solubility of the aggregate. "Concentration effect" of the nanoreactor resulted in the observed acceleration in reaction rate. Moreover, the remarkable enhancement of reaction rate might also be attributed to the phase-transfer capability of surfactant-type **catalyst 1**, which transported the real oxidant HClO from surrounding aqueous environment to hydrophobic core for faster catalysis. An unprecedented TOF value ($2.48 \times 10^3 \text{ h}^{-1}$) was achieved over

catalyst 1 in the aqueous epoxidation of styrene. The value was even significantly higher than that obtained over previously reported chiral salen Mn^{III} complexes in homogeneous or heterogeneous systems.^{41, 44-47} Furthermore, in the absence of the additive PyNO, the activity and enantioselectivity of **catalyst 1** apparently decreased, indicating that PyNO as an axial ligand had a pronounced effect on both the activity and the enantioselectivity of the asymmetric epoxidation reaction, which has been reported for other chiral salen Mn(III) catalysts (Table 1, entry 2).⁴¹

Table 1. Results of the enantioselective epoxidation of unfunctionalized olefins over different chiral salen Mn^{III} complexes in water^a

Entry	Catalyst	Substrate	Product	t (min)	Conv. ^b /%	ee ^b /%	TOF ^c × 10 ³ /h ⁻¹
1	Catalyst 1			3	99	39	2.48
2	Catalyst 1 ^d			3	45	27	1.13
3	neat complex		R	3	16	5	0.40
4	PNIPAAm			3	trace	/	/
5	Catalyst 1			3	48	49	1.20
6	Catalyst 1			30	99	75	/
7	neat complex			3	15	35	0.38
8	Catalyst 1			3	45	47	1.13
9	Catalyst 1			35	99	70	/
10	neat complex			3	12	40	0.30
11	Catalyst 1			3	40	51	1.00
12	Catalyst 1			45	99	77	/
13	neat complex			3	10	44	0.25
14	Catalyst 1			3	16	83	0.40
15	Catalyst 1			180	99	92	/
16	neat complex			3	3	78	0.08
17	Catalyst 1			3	14	80	0.35
18	Catalyst 1			200	99	94	/
19	neat complex			3	7	76	0.18

^a Catalyst (0.8 mol% of substrate, based on manganese ion content), substrate (0.25 mmol), pyridine *N*-oxide (0.5 mmol), NaClO (0.5 mmol, 0.5 M, pH = 11.5, added in one portion), water (1 mL), 2 °C. ^b Determined by GC. ^c TOF = (moles of substrate converted)/(moles of manganese centers) per hour, calculated from 3 min conversions. ^d Without PyNO.

To further understand the acceleration effect of **catalyst 1** in aqueous reaction systems, kinetics was used to study the reaction rates of asymmetric epoxidation of styrene over various amounts of **catalyst 1** in water. The catalyst amount was reduced from 0.8 to 0.1 mol%. Time-dependent plots of styrene conversion with various amount of **catalyst 1** were

shown in Fig. 8A. Both reactions in water reached equilibrium within 3 min. Notably, conversion of styrene was linearly increased up to 1 min, after which a significant increase was not observed. Therefore, the initial rate constant k_{obs} values were determined from the data within this time range. Detailed kinetic data for catalyst amount-dependence in water are given in Fig.

8C-a. Obviously, reaction rates decreased as reduction of catalyst amount in water, in terms of initial rate constants k_{obs} . By reducing **catalyst 1** from 0.8 to 0.4 mol%, the k_{obs} value decreased smoothly (Fig. 8C-a). It was logical that lower catalyst amount should reduce the total number of nanoreactors in solution and hence less “catalytic pumps” to catalyze the aqueous organic reaction. While, further lowering the catalyst amount to 0.2 mol%, led to a sharp decrease in k_{obs} value (Fig. 8C-a). In particular, a k_{obs} value of only 17.0 M/min was obtained when catalyst amount was reduced to 0.1 mol% (Fig. 8A-e). The collapse of reaction rate should be caused by the limited amount of available **catalyst 1** to form nanoreactor in water for confined catalysis. Therefore, **catalyst 1** self-assembles to form micelles in aqueous reaction systems when the amount is above 0.4 mol%.

Interestingly, this value (0.4 mol% of substrate in 2 mL solvent) agrees with the CMC (0.5 mmol.L⁻¹) of **catalyst 1**. Notably 0.8 mol% of **catalyst 1**-based micelles in water were sufficient for affording a quantitative conversion (99%) of styrene with a high ee value (39%) (Fig. 8A-a).

For comparison, we also used kinetics to study the reaction rates of asymmetric epoxidation of styrene over various amounts of **catalyst 1** in dichloromethane, as shown in Fig. 8B. Detailed kinetic data for catalyst amount-dependence in dichloromethane are presented in Fig. 8C-b. Notably, catalysis in dichloromethane was far less efficient than that in water, in terms of corresponding initial rate constants k_{obs} (Fig. 8C-b vs a). And the k_{obs} values in dichloromethane decreased smoothly as reduction of catalyst amount from 0.8 to 0.1 mol% (Fig. 8C-b). Actually, dichloromethane is a good solvent for the block of chiral salen Mn^{III} complex. Hence, **catalyst 1** containing hydrophilic PNIPAAm group and hydrophobic complex moiety may locate at the interface of water (aqueous NaClO) and dichloromethane in the biphasic system. Self-assembly into micelles didn't occur. **Catalyst 1** thus behaved as a common phase-transfer catalyst, rather than a concentrator. Lower local concentration of reagent and catalytic species in the common organic system was unfavorable for efficient catalysis.

Enhanced reaction rate over **catalyst 1** is also noticeable in the case of α -methylstyrene, indene, 1,2-dihydronaphthalene, 6-cyano-2,2-dimethylchromene, and 6-nitro-2,2-dimethylchromene, as shown by TOF in Table 1. **Catalyst 1** gave significantly higher TOF values than neat complex in corresponding epoxidations, due to the ability of the hydrophobic micelle cores to effectively sequester the organic substrates from the surrounding aqueous environment (Table 1, entry 5 vs. 7, entry 8 vs. 10, entry 11 vs. 13, entry 14 vs. 16, and entry 17 vs. 19). But unfortunately, **catalyst 1**-based nanoreactor showed substrate selectivity based on the size of substrates. Despite still unfunctionalized alkenes, bulkier alkenes were less reactive than styrene during aqueous asymmetric epoxidation (Table 1, entries 5, 8 and 11 vs. entry 1). In the presence of 0.8 mol% of **catalyst 1**, α -methylstyrene, indene, and 1,2-dihydronaphthalene gave only 40-48% conversions with unsatisfactory ee values. For more sterically hindered alkenes, such as 6-nitro-2,2-dimethylchromene and 6-cyano-2,2-dimethylchromene, even lower conversions (14-16%) were obtained during the reaction (Table 1, entries 14 and 17). While, the difference in reactivity of alkenes was not obvious when neat complex was used as the catalyst (Table 1, entries 3, 7,

10 and 13). This type of substrate selectivity should account for the selective shell permeability.⁴⁸ Nanostructured shell consisting of bulky PNIPAAm segments acted as size-exclusion gate of nanoreactor, which favored the penetration of small alkenes into the catalyst-containing micelle core for more efficient catalysis. In particular, substituted 2,2-dimethylchromene are solid and insoluble in water, which consequently have difficulty with permeating into hydrophobic core of nanoreactors for efficient catalysis (Table 1, entries 14 and 17). This gated permeability behavior makes **catalyst 1**-based micelle a selective nanoreactor for asymmetric epoxidation of alkenes in water. Notably, all alkenes used in this work get quantitatively oxidized to the corresponding epoxides with good to excellent enantioselectivity in water, in the case of prolonged reaction time (Table 1, entries 6, 9, 12, 15 and 18). The results suggested the flexibility of **catalyst 1** in green asymmetric epoxidation. It is the first successful example for efficiently performing asymmetric epoxidation of alkenes in pure water.

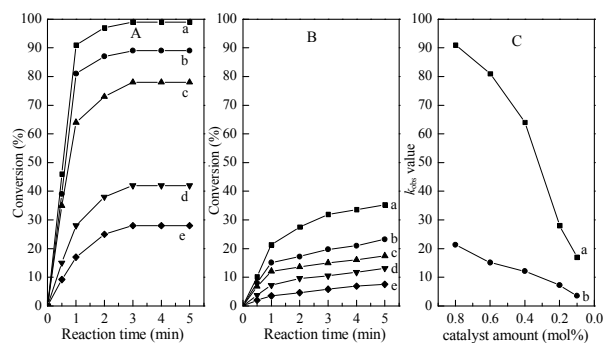


Fig. 8 Time-dependent plots of styrene conversion with various amounts of **catalyst 1** in water (A) and in dichloromethane (B) (catalyst amount based on manganese ion content: 0.8 mol% (a), 0.6 mol% (b), 0.4 mol% (c), 0.2 mol% (d), and 0.1 mol% (e)), and the detailed k_{obs} value for catalyst amount-dependence (C) in water (a) and in dichloromethane (b).

Recycling

Apart from its high efficiency, another salient feature of **catalyst 1** in water is its “smart” recovery. After each reaction, **catalyst 1** turned to a double hydrophobic block once heated above its LCST, leading to precipitation of catalyst for the next cycle. The aqueous phase was separated from the catalyst by decantation. Notably, although *n*-hexane was used to extract a small amount of epoxide from reaction solution in the present work, this approach was expected in large-scale industrial processes, in which the organic product phase can be directly separated from water without the use of any organic solvents. To our delight, **catalyst 1** could be reused for at least five times without significant loss of activity, as shown in Fig. 9.

Leaching tests to reaction medium were performed by directly determining the manganese content in supernatant *via* chemical analysis. No manganese was detected in the supernatant, which revealed the negligible leaching loss of manganese species during the reaction. Moreover, chemical analysis of the recovered catalyst gave manganese content (0.32 mmol/g) almost identical to that of the fresh one (0.33 mmol/g). FT-IR (see Fig. 1b vs b’), UV-vis (see Fig. 2b vs b’) and XPS (see Fig. 3b vs b’) spectra showed no significant change in catalyst even after the 5th reuse. Therefore, the efficient **catalyst 1** was stable under the basic

reaction condition (pH 11.5, NaClO buffer), and the axial N-Mn bonding remained intact during the epoxidation. Oxidative decomposition of chiral salen Mn^{III} complex, a main reason for deactivation of the complex in basic epoxidation,^{41, 49, 50} was avoided by localizing complex within a hydrophobic core. The possibility of formation of undesired inactive dimeric μ -oxo-manganese(IV) dimer,⁵¹ the cause for deactivation of the catalytic species, can also be prevented because of the bulky steric encumbrance of PNIPAAm on manganese center. Furthermore, mild reaction condition used in our studies, such as extremely short reaction time and low temperature, should potentially minimize catalyst degradation.

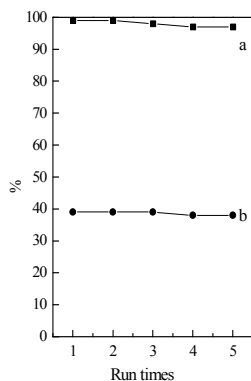


Fig. 9 Reuse of catalyst 1 in asymmetric epoxidation of styrene with NaClO as oxidant in water at 2 °C (a: conversion; b: ee value).

Conclusions

We have demonstrated the first asymmetric epoxidation of unfunctionalized olefins in pure water using a chiral salen Mn^{III} complex-based thermoresponsive nanoreactor. The nanoreactor with a hydrophobic catalytic core and a hydrophilic surface exhibited some distinct characteristics as follows: (a) hydrophobic core created a hydrophobic microenvironment with high local concentration of active sites and concentrated substrates, confining the asymmetric epoxidation for efficient catalysis; (b) hydrophilic surface guaranteed water-solubility of the nanoreactor, circumventing the limited mass transfer associated with aqueous organic reaction. Furthermore, the thermoresponsivity of nanoreactor facilitated the recovery of catalyst from reaction system by simply adjusting local temperature. The chiral salen Mn^{III} complex-based nanoreactor thus showed extremely high catalytic efficiency and steady reusability in asymmetric epoxidation of unfunctionalized olefins in water without need for any organic solvents. The advantages allow for industrial practice of the asymmetric epoxidation of unfunctionalized alkenes, and also raise the prospect of making water a viable environmentally friendly medium for organic synthesis.

Acknowledgements

The work was supported by the National Natural Science Foundation of China (Grant No. 21476069, 21003044), the Scientific Research Fund of Hunan Provincial Education Department (13B072), the Program for Excellent Talents in Hunan Normal University (ET14103), the Program for Science

and Technology Innovative Research Team in Higher Educational Institutions of Hunan Province, the Foundation for Innovative Research Groups of the Hunan Natural Science Foundation of China, the Construct Program of the Key Discipline in Hunan Province.

References

- W. Zhang, J. L. Loebach, S. R. Wilson and E. N. Jacobsen, *J. Am. Chem. Soc.*, 1990, **112**, 2801.
- S. Liao and B. List, *Angew. Chem. Int. Ed.*, 2009, **48**, 1.
- S. Liao and B. List, *Angew. Chem. Int. Ed.*, 2010, **49**, 628.
- F. Song, C. Wang and W. Lin, *Chem. Commun.*, 2011, **47**, 8256.
- R. Luo, R. Tan, Z. Peng, W. Zheng, Y. Kong and D. Yin, *J. Catal.*, 2012, **287**, 170.
- S. Shabbir, Y. Lee and H. Rhee, *J. Catal.*, 2015, **322**, 104.
- B. E. Hanson, *Coord. Chem. Rev.*, 1999, **185-186**, 795.
- U.M. Lindstrom, *Chem. Rev.*, 2002, **102**, 2751.
- J. Tan, H. Li and Y. Gu, *Green Chem.*, 2010, **12**, 1772.
- P. Cotanda, A. Lu, J. P. Patterson, N. Petzetakis and R. K. O'Reilly, *Macromolecules*, 2012, **45**, 2377.
- Y. Kong, R. Tan, L. Zhao and D. Yin, *Green Chem.*, 2013, **15**, 2422.
- Y. Jung and R. A. Marcus, *J. Am. Chem. Soc.* 2007, **129**, 5492.
- A. Chanda and V. V. Fokin, *Chem. Rev.*, 2009, **109**, 725.
- T. Dwars, E. Paetzold and G. Oehme, *Angew. Chem., Int. Ed.*, 2005, **44**, 7174.
- S. Luo, X. Mi, S. Liu, H. Xu and J. Cheng, *Chem. Commun.*, 2006, 3687.
- V. Rauniyar, A. D. Lackner, G.L. Hamilton and F.D. Toste, *Science*, 2011, **334**, 1681.
- K. Manabe, S. Iimura, X. Sun and S. Kobayashi, *J. Am. Chem. Soc.*, 2002, **124**, 11971.
- Y. Wang, H. Xu, N. Ma, Z. Wang, X. Zhang, J. Liu and J. Shen, *Langmuir*, 2006, **22**, 5552.
- J. Li, Y. Tang, Q. Wang, X. Li, L. Cun, X. Zhang, J. Zhu, L. Li and J. Deng, *J. Am. Chem. Soc.*, 2012, **134**, 18522.
- A. Lu and R. K. O'Reilly, *Current Opinion in Biotechnology*, 2013, **24**, 639.
- Y. Liu, Y. Wang, Y. Wang, J. Lu, V. Piñón, III, and M. Weck, *J. Am. Chem. Soc.*, 2011, **133**, 14260.
- T. Sun and G. Qing, *Adv. Mater.*, 2011, **23**, 57.
- T. Sun, G. Qing, B. Sua and L. Jiang, *Chem. Soc. Rev.*, 2011, **40**, 2909.
- V. B. Schwartz, F. Thétiot, S. Ritz, S. Pütz, L. Choritz, A. Lappas, R. Förch, K. Landfester and U. Jonas, *Adv. Funct. Mater.*, 2012, **22**, 2376.
- F. Hapiot, S. Menuel, E. Monflier, *ACS Catal.* 2013, **3**, 1006.
- J. E. Chung, M. Yokoyama, T. Aoyagi, Y. Sakurai and T. Okano, *J. Controlled Release*, 1998, **53**, 119.
- J. F. Larrow, E. N. Jacobsen, Y. Gao, Y. P. Hong, X. Y. Nie and C. M. Zepp, *J. Org. Chem.*, 1994, **59**, 1939.
- B. Rößbach, K. Leopold and R. Weberskirch, *Angew. Chem. Int. Ed.*, 2006, **45**, 1309.
- B. Gall, M. Bortenschlager, O. Nuyken and R. Weberskirch, *Macromol. Chem. Phys.* 2008, **209**, 1152.
- M. J. Monteiro, *Macromolecules*, 2010, **43**, 1159.
- M. J. Monteiro, *Macromolecules*, 2010, **43**, 9598.
- F. Tu and D. Lee, *J. Am. Chem. Soc.*, 2014, **136**, 9999.
- C. Baleizão and H. Garcia, *Chem. Rev.* 2006, **106**, 3987.
- W. Chen, Y. Sung, C. Chang, Y. Chen and M. Ger, *Surf. Coat. Technol.*, 2010, **204**, 2130.
- L. Lou, K. Yu, F. Ding, X. Peng, M. Dong, C. Zhang and S. Liu, *J. Catal.*, 2007, **249**, 102.
- R. Tan, D. Yin, N. Yu, H. Zhao and D. Yin, *J. Catal.*, 2009, **263**, 284.
- R. Luo, R. Tan, Z. Peng, W. Zheng, Y. Kong and D. Yin, *J. Catal.* 2012, **287**, 170.
- J. Huang, X. Fu and Q. Miao, *Appl. Catal. A*, 2011, **407**, 163.

- 39 J. Huang, X. Fu, C. Wang, H. Zhang and Q. Miao, *Microporous Mesoporous Mater.*, 2012, **153**, 294.
- 40 A. R. Silva, K. Wilson, J. H. Clark and C. Freire, *Microporous Mesoporous Mater.*, 2006, **91**, 128.
- 5 41 B. Gong, X. Fu, J. Chen, Y. Li, X. Zou, X. Tu, P. Ding and L. Ma, *J. Catal.*, 2009, **262**, 9.
- 42 G. Liu, W. Fan, L. Li, P.K. Chu, K.W.K. Yeung, S. Wu and Z. Xu, *J. Fluorine Chem.*, 2012, **141**, 21.
- 43 M. Li, S. Qi, Y. Jin, W. Yao, S. Zhang, and J. Zhao, *Colloids Surf., B*, 2014, **123**, 852.
- 10 44 R. Tan, D. Yin, N. Yu, Y. Jin, H. Zhao and D. Yin, *J. Catal.*, 2008, **255**, 287.
- 45 N. Ch. Maity, S. H. R. Abdi, R. I. Kureshy, N. H. Khan, E. Suresh, G. P. Dangi and H. C. Bajaj, *J. Catal.*, 2011, **277**, 123.
- 15 46 R. I. Kureshy, T. Roy, N. H. Khan, S. H. R. Abdi, A. Sadhukhan and H. C. Bajaj, *J. Catal.*, 2012, **286**, 41.
- 47 Y. Chen, R. Tan, Y. Zhang, G. Zhao, W. Zheng, R. Luo and D. Yin, *Appl. Catal., A*, 2015, **491**, 106.
- 48 W. Meier, *Adv. Funct. Mater.*, 2011, **21**, 1241.
- 20 49 Z. Xu, X. Ma, Y. Ma, Q. Wang and J. Zhou, *Catal. Commun.*, 2009, **10**, 1261.
- 50 W. Zheng, R. Tan, S. Yin, Y. Zhang, G. Zhao and D. Yin, *Catal. Sci. Technol.*, 2015, **5**, 2092.
- 51 C. E. Song, *Annu. Rep. Prog. Chem., Sect. C*, 2005, **101**, 143.

25

Graphical Abstract

Asymmetric epoxidation of unfunctionalized olefins accelerated by thermoresponsive self-assemblies in aqueous system

Yaoyao Zhang,^a Rong Tan,^{*a} Guangwu Zhao,^a Xuanfeng Luo,^a and Donghong Yin^{*a,b}

^a Key Laboratory of Chemical Biology and Traditional Chinese Medicine Research (Ministry of Education),

Key Laboratory of the Assembly and Application for Organic Functional Molecules, Hunan Normal

University, Changsha, Hunan, 410081, China;

^b Technology Center, China Tobacco Hunan Industrial Corporation, NO. 426 Laodong Road, Changsha,

Hunan, 410014, China.

Thermoresponsive self-assembled nanoreactor, comprising a hydrophilic PNIPAAm shell and a hydrophobic chiral salen Mn^{III} complex core, exhibits unprecedented efficiency and facile reusability in asymmetric epoxidation of unfunctionalized olefins in pure water without using any organic solvents.

